

An experimental study on different socket base connections under cyclic loading

Selim Pul*, Metin Hüsem, Mehmet Emin Arslan and Sertaç Hamzaçebi

Karadeniz Technical University, Department of Civil Engineering, 61080, Trabzon, Turkey

(Received November 14, 2012, Revised August 7, 2013, Accepted September 16, 2013)

Abstract. This paper presents an experimental study on socket base connections of precast reinforced concrete columns. The main purpose of this study is to determine socket base connection which has the closest behavior to monolithic casted column-base joints. For this purpose, six specimens having different column-socket base connection details were tested under cyclic loading. For each test, strength, stiffness, ductility and drift ratios of the specimens were determined. Test results indicated that a suggested connection type is 10% - 30% stronger than the other type of connections under lateral loading. The welded connection (PC-5) had better lateral load carrying capacity and ductility. On the other hand, performance of standard connection (PC-1) which is commonly used in construction was weaker than other connections. Thus, decision of connection type should be referred not only performance but also applicability.

Keywords: precast columns; socket base connection; cyclic loading; energy dissipations; stiffness degradation; displacement ductility

1. Introduction

It is known that the main function of columns is to transfer vertical and lateral loads to ground through foundations safely. This is very critical for the structural stability. For monolithic casted reinforced concrete structures, it is easier to obtain this behavior than those of precast structures. This is because; it is difficult to constitute moment resisting connections for precast members.

Many studies have been carried out on monolithic reinforced concrete structures under seismic effects. Since precast construction includes different connection details for each structural member, results of these studies do not reflect entirely behavior of precast concrete structures. In recent years, several studies conducted on precast structural members to determine the behavior of precast connections. Blakeley and Park (1971), examined the behavior of beam-to-column connections, connected, post-tensioning, with anchorage and partial anchorage (Kaya and Arslan 2009a). Park and Thompson (1997) tested ten column-to-beam connections in which mild steel and high strength reinforcing bars were used for the post-tensioning. In addition, several parameters were tested in a study at NIST (U.S. National Institute of Standards and Technology) (Cheok and Lew 1991, Cheok and Lew 1993, Cheok *et al.* 1994).

*Corresponding author, Professor, E-mail: spul@ktu.edu.tr

2. Experimental

2.1 Material properties

Specimens were produced by using limestone aggregate CEM II/B-M (P-LL) 32.5R was used as cement and dosage was kept constant at 350 kg/m^3 with water to cement ratio of 0.5. Mixture proportion of the concrete is given in Table 1.

Characteristic compressive strength of the concrete used for producing columns and bases is 27.4 MPa and the yield strength values of 8 and 14 mm diameter steel bars are 536 MPa and 539 MPa, respectively.

2.2 Properties of the specimens

The main purpose of this study was to investigate lateral loading behavior of column-base connections. For this purpose the tests were carried out on five different column-base connection specimens and one monolithic reinforced concrete column-base joint for comparison under lateral cyclic loading. Dimension and reinforcement details of the half scale specimens are given in Fig. 1. Connection details of test specimens are given in Fig. 2. PC-1 (Standard Connection) is the most commonly used socket base connection type. In this connection, precast column member was embedded into the 200 mm deep socket. The gap between socket and column was filled with high quality, 40 MPa compressive strength mortar. PC-2 is an anchored connection. As it is seen in Fig. 2, two holes were left in the column to connect M20 bolts and 100.100.7 angles together. Two M20 bolts through the holes in column were connected the angles. Afterwards, 100.100.7 angles were

Table 1 Mix proportions of concrete

W/C Ratio	Mixing water (kg/m^3)	Cement (kg/m^3)	Saturation water (kg/m^3)	Aggregate (kg/m^3)
0.5	175	350	28	1864

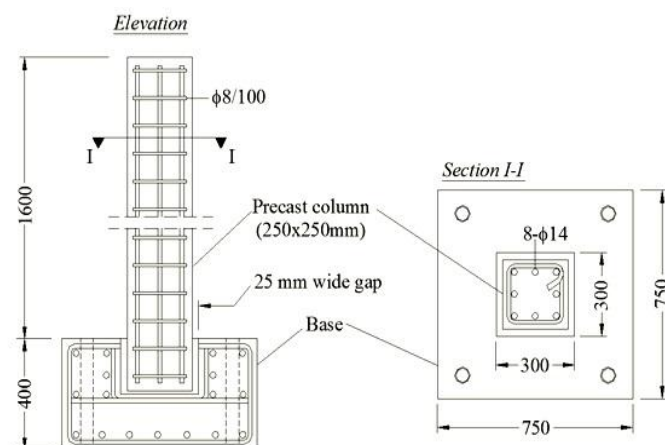


Fig. 1 Dimensions and reinforcement details of specimens (dimensions are in mm)

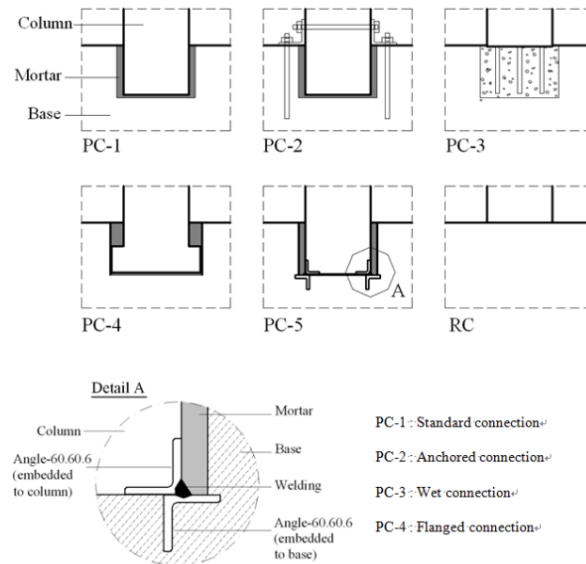


Fig. 2 Connection details of specimens

anchored to the base with three M20 stud bolts. PC-3 is a wet connection. In this connection, socket within the base filled with fresh concrete and column having 20 cm development length at the bottom embedded into cavity. PC-4 is flanged connection. Flanges were constituted at the bottom of the precast column and after placing column socket was filled with high quality mortar. The last connection PC-5 is a welded connection. This connection was constructed by welding 60.60.6 angles in base and at the bottom of column together and again socket was filled with high quality mortar. To compare the results of the connections a reference monolithic reinforced concrete column base joint (RC) was produced.

2.3 Test setup and instrumentation

The test setup and instrumentation are given in Fig. 3. The foundations of test specimens were anchored to the strong floor. A servo-hydraulic actuator (force rating: 280 kN; max. stroke: 200 mm) was used to apply reversed cyclic lateral displacement to the test specimens. Applied loading protocol used in the study is given in Fig. 4. Lateral loads and top displacements were measured by means of a 50kN capacity load-cell and 200 mm capacity LPDT, respectively. These values were recorded by using a data logger acquisition system to the computer.

3. Experimental results

The cracking pattern was monitored throughout the tests and useful information was provided regarding the failure mechanism for each specimen (Xue and Yang 2010). Fig. 5 shows failure behavior of specimens at column-base connection observed at the end of tests. Lateral load–displacement hysteretic curves of the test specimens are shown in Fig. 6.

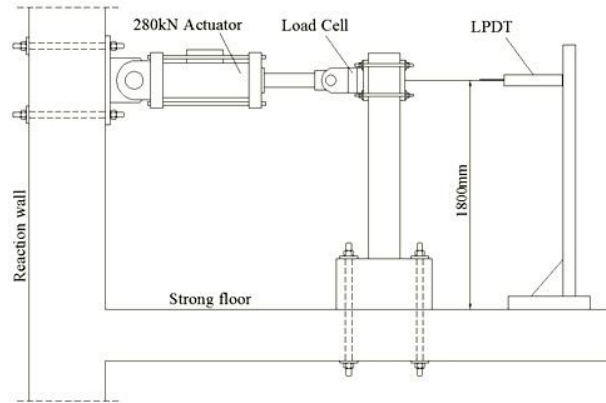


Fig. 3 Test setup

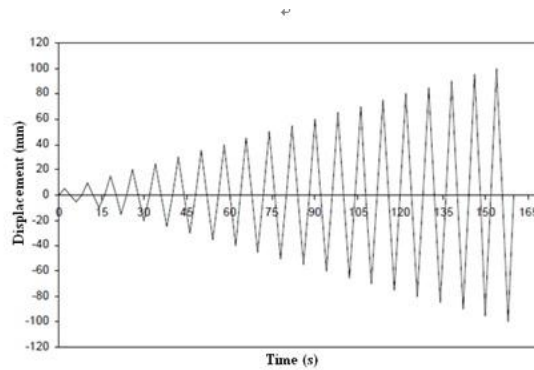


Fig. 4 Loading protocol

Specimen PC-1

Failure occurred approximately 50 mm below of the base top level and plastic hinge occurred at this point for specimen PC-1 which represents standard socket base connection. On the other hand, column was compelled to slip from the base by lateral cyclic loading. Maximum slip value was measured as 6 mm. Failure shape indicates that cyclic loading caused loss of bond by crushing the mortar between the cavity and the column. At a drift ratio of 1.37%, PC-1 specimen reached the yield state that was defined according to the criteria used by Park (1989) for equivalent elastoplastic energy absorption and its maximum load-carrying capacity (30.17 kN) at a drift ratio of 2.37%. At 3.5% drift ratio specimen approximately 22 kN load carried.

Specimen PC-2

The cracks were observed throughout the column but no slippage occurred. Plastic hinge occurred on column above the base surface around the holes which were left for connecting bolts and plates. At a drift ratio of 2.12%, PC-2 specimen reached the yield state and its maximum load-carrying capacity (44.93 kN) at a drift ratio of 3.19%. The specimen carried in the vicinity of 44 kN load at the drift ratio of 3.5%.

Specimen PC-3

PC-3 had wet connection. Failure happened crushing of filling concrete placed into the cavity

to connect column and base. In addition, development length fell short and slipping occurred, thus load carrying capacity decreased. For the specimen, drift ratio at yield state and maximum load (36.45 kN) are 1.92% and 2.47%, respectively. Load level on the column at the drift ratio of 3.5% was around 28 kN.

Specimen PC-4

PC-4 has similar failure shape and load carrying capacity with PC-3 specimen, but by the help of flange placed bottom of column prevented slipping and contribute stiffness of precast column. At yield state specimen has 1.28% drift ratio and its maximum load-carrying capacity (35.19 kN) at a drift ratio of 2.37%. At 3.5% drift ratio specimen approximately 30 kN load carried.

Specimen PC-5

PC-5 was the last connection constructed by welding L60.60.6 plates in base and at the bottom of column together and afterwards cavity was filled with high quality mortar. This connection has the closest behavior to RC specimen. At a drift ratio of 2.13%, PC-5 specimen reached the yield state and its maximum load-carrying capacity (44.99 kN) at a drift ratio of 2.81%. The specimen carried about 43 kN load at the drift ratio of 3.5%.

Specimen RC

RC was the reference specimen. As it was expected, the specimen showed the best performance. Failure pattern of the specimen is quite similar with PC-5 specimen. At yield state specimen has 1.86% drift ratio and its maximum load-carrying capacity (44.62 kN) at a drift ratio of 2.73%. At 3.5% drift ratio specimen approximately 43 kN load carried.

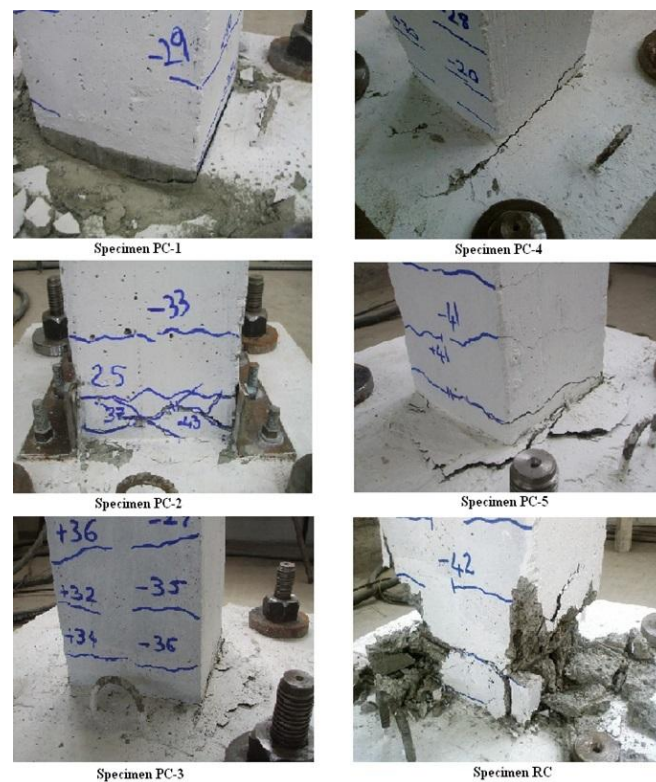


Fig. 5 Failure behavior of specimens at column-base connection

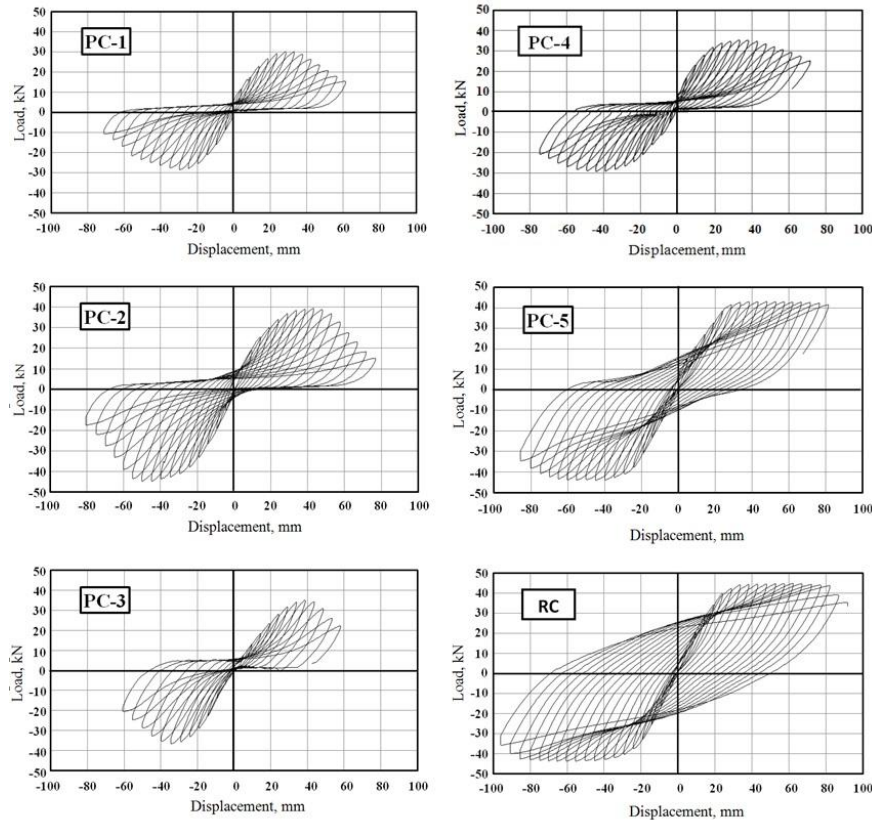


Fig. 6 Lateral load–displacement hysteretic curves of the specimens

4. Discussion of test results

4.1 Strength and stiffness degradations

The average load carrying capacities of test specimens are given in Fig. 7. PC-1 (standard connection) which is commonly used in construction has the lowest load carrying capacity. This result should be considered again for application of the connection. RC specimen had higher load carrying capacity and it was followed by PC-5 specimen. Envelope curves of test specimens are summarized in Fig. 8.

Stiffness degradation is a parameter used to evaluate the specimen's overall response. In order to assess stiffness degradation, the secant stiffness was computed for each loading cycle at a particular drift level. The secant stiffness was calculated using a straight line between the maximum load and corresponding displacement points for the positive and negative directions in a load cycle. Stiffness degradation-drift ratio curves of the specimens are given in Fig. 9. It is clearly seen from the curve, stiffness continuously decreases with increasing drift ratio, because cumulative damage in columns increases throughout the test. In addition each specimen experienced severe stiffness degradation at the end of the test.

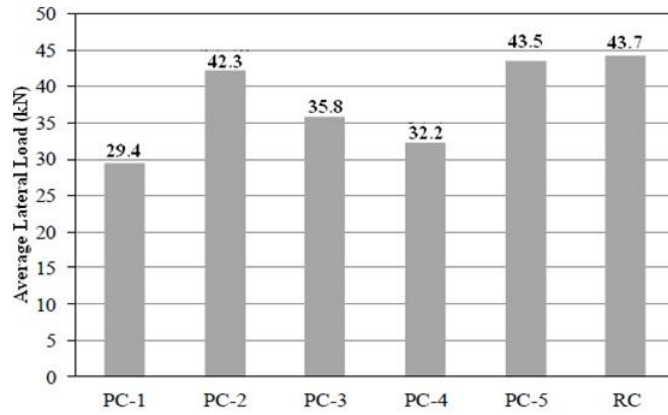


Fig. 7 Average load carrying capacities of the specimens

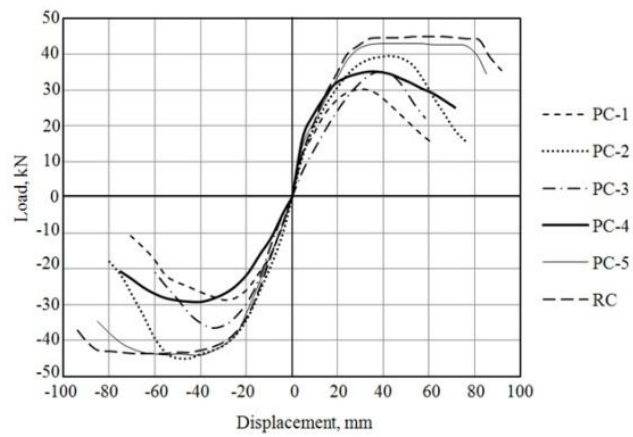


Fig. 8 Envelopes of lateral load–displacement curves

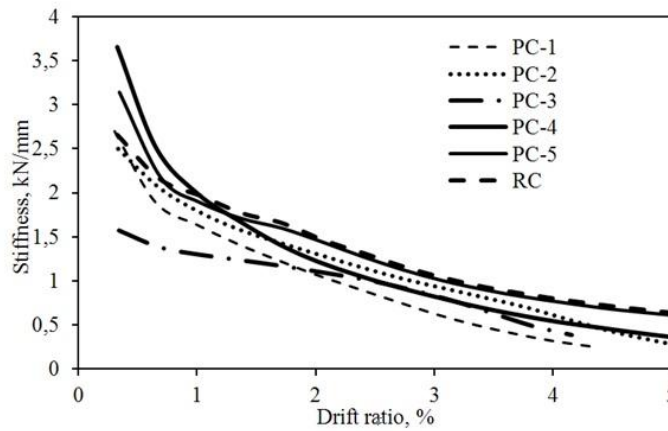


Fig. 9 Stiffness degradation of the specimens

4.2 Displacement ductility

The displacement ductility is the ratio of the maximum deformation that a structure or element can undergo without a significant loss of initial yielding resistance to the initial yield deformation. However, it was not easy to determine yield points for the specimens directly from the lateral load–displacement curves. For each specimen, the load–displacement envelope curve was used to define the yield and maximum displacements according to the criteria for equivalent elastoplastic energy absorption used by Park (1989) and Xue and Yang (2010) (Fig. 10). The ultimate displacement Δ_u corresponded to a 15% drop of the peak load. The displacement ductility was calculated from the ratio of ultimate displacement to yield displacement Δ_u / Δ_y . Displacements at yield, maximum and ultimate loads and displacement ductility of test specimens are shown in Table 2. The average displacement ductility of specimens PC- 1, PC-2, PC-3, PC-4, PC-5 and RC are 2.31, 2.13, 1.69, 2.92, 3.05 and 3.28, respectively.

These results show that PC-5 (welded connection) has similar behavior with RC sample and higher displacement ductility than those of other connection types. However PC-3 (wet connection) has the lowest displacement ductility. It is thought that this result stems from slipping of steel bars due to insufficient development length and unavailability of bars to splice column reinforcements for anchorage.

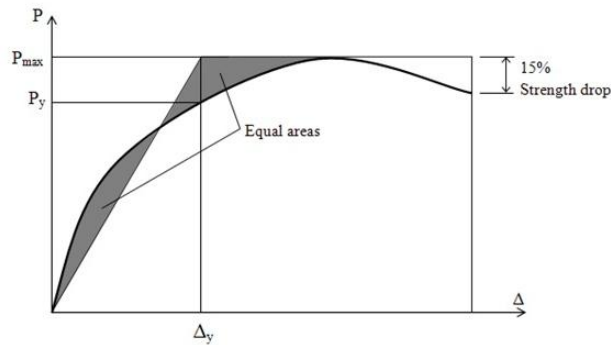


Fig. 10 Determination of yield and ultimate displacements

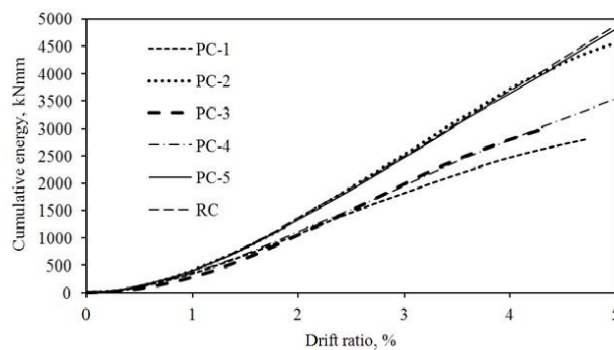


Fig. 11 Cumulative energy dissipations of the specimens

4.3 Energy dissipation capacity

The cumulative energy dissipations of the specimens at a particular drift ratio are shown in Fig. 11. Specimen PC-2, PC-5 and RC showed similar energy dissipation. Also energy dissipation of PC-1, PC-3 and PC-4 increased parallel to each other until 2.5% drift ratio. After this drift ratio energy dissipation of PC-1 specimen slightly decreased corresponding to PC-3 and PC-4 specimens.

This result proves that PC-1 specimen shows less ductile behavior and has lower displacement and load carrying capacity. During the initial cycles of tests specimens were in elastic stage and dissipated energies were small. At elastoplastic stage, energy dissipation increased with increasing damage. After reaching the peak load, the load-carrying capacity of the test specimens began to gradually decrease, but the energy-dissipation capacity still slowly increased.

5. Conclusions

The main purpose of this study was to investigate behavior of different socket base connections and determine the connection showing the closest behavior to the monolithic column-base joints. For this purpose, five different column base connections designed, constructed and tested under lateral cyclic loading. Based on the test results of this study, the following conclusions can be made:

- As it was expected RC specimen had higher load carrying capacity and it was followed by PC-5 specimen. PC-1 (standard connection) which is commonly used in construction has the lowest load carrying capacity. This result should be considered again for application of the connection. Load carrying capacities of PC-5, PC-2, PC-3, PC-4 and PC-1 socket base connection specimens are lower 0.5%, 3.2%, 18.1%, 26.3% and 32.7% than that of RC specimen, respectively.

- RC specimen showed the most ductile behavior when the average displacement ductility was considered. The average displacement ductility of specimens PC-5, PC-4, PC-1, PC-2 and PC-3 are lower 7.0%, 11.0%, 29.6%, 35.1% and 48.5% than that of RC specimen, respectively.

- Specimen PC-2, PC-5 and RC have almost the same energy dissipation capacity at 3.5%. Also energy dissipation of PC-1, PC-3 and PC-4 increased parallel to each other until 2.5% drift ratio. After this drift ratio energy dissipation of PC-1 specimen slightly decreased corresponding to PC-3 and PC-4 specimens.

- PC-4 has similar failure shape and load carrying capacity with PC-3 specimen, but by the help of flange prevented slipping and contributed stiffness and ductility of the specimen. This result proves effectiveness of flange.

- Although PC-2, PC-5 and RC specimens have almost the same load carrying capacity, it is clearly seen from the envelope curves that PC-5 and RC specimen show more ductile manner. When strength, stiffness, ductility and energy dissipation were evaluated together to determine the closest behavior to the RC specimen, PC-5 showed the best performance.

- The performances of PC-1, PC-3 and PC-4 aren't satisfying corresponding to PC-2 and PC-5 specimens, even if their applications are easy.

Consequently, connections were designed based on the engineering judgment and common sense rather than the code specifications, because of limited knowledge about socket base connections. Fortunately, very positive results were obtained after the tests. The test results were

evaluated by considering strength, stiffness and ductility of the specimens together and the best performance was determined. However, it should be expressed that results and conclusions are based on the concrete class, members and test conditions. Thus, it will be useful for precast construction industry to repeat similar experiments by using different connections under varied conditions.

References

- Alyavuz, B. and Anıl, Ö. (2007), "Nonlinear finite element analysis of loading transferred from column to socket base", *J. Fac. Eng. Arch. Gazi Univ.*, **22**(3), 471-479.
- American Concrete Institute (ACI) Committee 318, (2008), *Building Code Requirements for Structural Concrete (ACI 318-08) and Commentary (ACI 318R-08)*, Farmington Hills, MI: ACI.
- Bhatt, P. and Kirk, D.W. (1985), "Tests on an improved beam column connection for precast concrete", *ACI J.*, **82**(6), 834-843.
- Blakeley, R.W. and Park, R. (1971), "Seismic resistance of prestressed concrete beam-column assemblies", *ACI J.*, **68**(9), 677-692.
- Campos, G.M., Canha, R.M.F. and EL DEBS, M.K. (2011), "Design of precast columns bases embedded in socket foundations with smooth interfaces", *Ibarcon Struct. Mater. J.*, **4**(2), 304-323.
- Canha, R.M.F., Jaguaribe, K.B., El Debs, A.L.H.C. and El Debs, M.K. (2009a), "Analysis of the behavior of transverse walls of socket base connections", *Eng. Struct.*, **31**, 788-798.
- Canha, R.M.F., Ebeling, E.B., El Debs, A.L.H.C. and El Debs, M.K. (2009b), "Analysing the base of precast column in socket foundations with smooth interfaces", *Mater. Struct.*, **42**(6), 725-737.
- Cheok, G.S. and Lew, H.S. (1991), "Performance of precast concrete beam-to-column connections subject to cyclic loading", *PCI J.*, **36**(3), 56-67.
- Cheok, G.S. and Lew, H.S. (1993), "Model precast concrete beam-to-column connections subject to cyclic loading", *PCI J.*, **38**(4), 80-92.
- Cheok, G.S., Stanton, J.F. and Seagren, D. (1994), "Beam-to-column connections for precast concrete moment resisting frames", *Proceeding of the 4th Joint Technical Coordinating Committee*, May 16-17, Tsukuba, Japan.1-8.
- Ertaş, O. and Özden, Ö. (2007), "Ductile connections in pre-cast concrete moment resisting frames", *Sixth National Conference on Earthquake Engineering*, 16-20 October 2007, Istanbul, Turkey.
- Hawileh, R.A., Rahman, A. and Tabatabai, H. (2010), "Nonlinear finite element analysis and modeling of a precast hybrid beam-column connection subjected to cyclic loads", *Appl. Math. Model.*, **34**, 2562-2583.
- FIB (2003), *International Federation of Precast Concrete Building Structures*, Lausanne, Switzerland
- Kaya, M. and Arslan, S. (2009a), "The effect of the diameter of prestressed strands providing the post-tensioned beam-to-column connections", *Mater. Des.*, **30**, 2604-2617.
- Kaya, M. and Arslan, S. (2009b), "Analytical modeling of post-tensioned precast beam-to-column connections", *Mater. Des.*, **30**, 3802-3811
- Khaloo, A.R. and Parastesh, H. (2003), "Cyclic loading of ductile precast concrete beam-column connection", *ACI Struct. J.*, **3**, 440-445.
- Korkmaz, H.H. and Tankut, T. (2005), "Performance of a precast concrete beam-to-beam connection subject to reversed cyclic loading", *Eng. Struct.*, **27**, 1392-1407.
- Leonhardt, F. and Mönnig, E. (1973), "Vorlesungen über massivbau", Berlin: Springer-Verlag.
- Osanai, Y., Watanabe, F. and Okamoto, S. (1996), "Stress transfer mechanism of socket base connections with precast concrete columns", *ACI Struct. J.*, **93**(3), 266-276.
- Park, R. (1989), "Evaluation of ductility of structures and structural assemblages from laboratory testing", *Bulletin of the New Zealand National Society for Earthquake Engineering*, **22**(3), 55-166.
- Park, R. and Thompson, K.J. (1997), "Cyclic load tests on prestressed beam column joints", *PCI J.*, **22**(5), 84-110.

- Pillai, S.U. and Kirk, D.W. (1981), "Ductile beam-column connection in precast concrete", *ACI J.*, **8**(6), 480-487.
- Priestly, M.J.N. and Tao, J.R. (1997), "Seismic response of precast prestressed concrete frames with partially debonded tendons", *PCI J.*, **38**(1), 58-68.
- Priestly, M.J.N. and McRae, J.R. (1996), "Seismic tests of precast beam-to-column joint subassemblages with unbonded tendons", *PCI J.*, **41**(1), 64-80.
- Xue, W. and Yang, X. (2010), "Seismic tests of precast concrete, moment resisting frames and connections", *PCI J.*, Summer 102-121.

CC